JOURNAL OF Applied Polymer SCIENCE

Synthesis and Characterization of *In Situ* Polymerized Poly(methyl methacrylate)-Cerium Molybdate Nanocomposite for Electroanalytical Application

Asif Ali Khan, Leena Paquiza

Faculty of Engineering and Technology, Department of Applied Chemistry, Analytical and Polymer Research Laboratory, Aligarh Muslim University, Aligarh 202002, India

Correspondence to: A. A. Khan (E-mail: asifkhan42003@yahoo.com) or L. Paquiza (E-mail: leenaz1@rediffmail.com)

ABSTRACT: In the present study, a new technique to synthesize composites of poly(methyl methacrylate) cerium molybdate (PMMA–CeMoO4) is reported. The study concerns the characterization of poly(methyl methacrylate; PMMA) and PMMA–$CeMoO_4$ nanocomposites are also discussed. The physical properties of the material were described using TGA–DTA, FTIR, X-ray, TEM, and SEM studies. The adsorption efficiency towards heavy metal ions was determined by distribution studies and material was found to be highly selective for lead, a heavy toxic metal ion, indicating the utility of the synthesized material for the removal of this ion from the waste stream. The material was used as electroactive component for the construction of an ion-selective membrane electrode. The membrane electrode was mechanically stable, having wide dynamic range, with quick response time and could be operated for at least 5 months without any considerable divergence in the potential response characteristics. The electrode was successfully used as indicator electrode in complexation titrations. © 2012 Wiley Periodicals, Inc. J. Appl. Polym. Sci. 000: 000–000, 2012

KEYWORDS: PMMA; polymerization; lead-selective electrode; potentiometry; hybrid composite; cerium molybdate

Received 5 July 2011; accepted 11 March 2012; published online 00 Month 2012
DOI: 10.1002/app.37672

INTRODUCTION

The hybrid nanocomposite materials have been studied in recent years, with the expectation that nanocomposite materials will serve as an important and evolutionary means of achieving properties that cannot be realized with single materials.[1–3] Because of the excellent properties, synergistically derived from polymer and inorganic materials, polymeric–inorganic composite materials are used in many fields.[4] The hybrid composite materials with nanoscale domains show unique chemical and physical properties that are different from composites with micro scale domains.[5,6] These materials are generally prepared by incorporating covalent bonds[7–11] or by physical interactions[12–15] to improve the compatibility between organic and inorganic phases.

Molecular level combination between organic polymers as supporting materials and inorganic precipitates of polyvalent metal acid salts as ion-exchanger prepared by "sol–gel" method has been of great interest in our laboratory.[16–20] The sol–gel route provides a useful method to prepare inorganic and organic–inorganic hybrid materials for use in chemical analysis. The inherent usefulness of this approach is largely due to the ease at which sol–gel-derived materials can be prepared, modified, and processed. Applications of these materials have been explored in the fields of catalyst,[21,22] coatings,[23] gas perm selectivity,[24] fuel cell,[25–27] chemical sensors, and ion exchange.[28,29] In this article, we propose a new method to prepare composite using poly (methyl methacrylate; PMMA) by free radical suspension polymerization using water as a medium, with *in situ* "sol–gel" transformation.[30] The literature survey revealed that still composite of PMMA, as cation exchanger, is not prepared by this method. The morphology, structural properties and thermal behavior of PMMA–$CeMoO_4$ nanocomposite polymer is discussed here.

PMMA is one of the earliest glassy polymers and is well known around the world by a variety of trade names Lucite, Oroglas, Perspex, and Plexiglas. It is an excellent material because of its potential application in optical fibers and high environmental stability compared to other plastics such as polycarbonate. Health effects are minimal for PMMA.

When PMMA is combined with inorganic material, the resulting hybrid material shows high thermal stability[31,32] and selectivity thus used in fabrication of ion selective electrode for

Table I. Conditions of Preparation and the Ion-Exchange Capacity of Various Sample of PMMA–$CeMoO_4$ Composite Cation Exchanger

	Mixing volume ratios (v/v)								
Sample no.	0.1*M* Ceric ammonium nitrate in DMW	0.1*M* Ammonium molybdate in DMW	pH of inorganic precipitate	MMA	BPO	PVA	Na_2HPO_4	Appearance after drying	I.E.C. (mequiv/g)
S-1	0.5	1	1.0	1	0.01	0.03	0.25	Pale yellow granules	0.40
S-2	0.5	1.5	1.0	1	0.01	0.03	0.25	Pale yellow granules	0.55
S-3	0.5	2	1.0	1	0.01	0.03	0.25	Pale yellow granules	0.67
S-4	1	2	1.0	1	0.01	0.03	0.25	Pale yellow granules	0.98
S-5	0.5	3	1.0	1	0.01	0.03	0.25	Pale yellow granules	1.18
S-6	**1**	**3**	**1.0**	**1**	**0.01**	**0.03**	**0.25**	**Pale yellow granules**	**1.60**
S-7	1	3	1.0	-	-	-	-	Yellow granules	1.45

sensing lead ions. The sensor was compared with few other Pb^{2+} ion selective electrodes reported in the literature.[33–36]

Lead in general is a metabolic poison, enzyme inhibitor and a suspected carcinogen. It causes damage to the nervous systems and kidneys. Though, there are a number of methods devised for the determination of Pb^{2+} ions such as spectrophotometry, polorography, atomic absorption spectrometry, and HPLC. Such methods, however, require a good infrastructure development, maintenance, and adequate expertise whereas ion selective electrode provide simple, cheap, and easy to use device for analysis of heavy metal ions. The proposed sensor exhibit significantly high sensitivity, stability, and selectivity for Pb^{2+} ions over many common ions, thus used for determining Pb^{2+} ions in various matrices successfully.

EXPERIMENTAL

Reagents and Instruments

Methyl methacrylate (MMA) monomer supplied by Merck, was purified by distillation under a vacuum. Benzoyl peroxide (BPO) (Loba Chemicals, India) was used as an initiator while polyvinyl alcohol (PVA) and anhydrous di-sodium hydrogen phosphate (Na_2HPO_4) were used from Aldrich and CDH, India, respectively. Ceric ammonium nitrate $[(NH_4)_2{\cdot}Ce(NO_3)_6]$ (BDH, India) and ammonium molybdate, $[(NH_4)_6Mo_7O_{24}{\cdot}4H_2O]$ (BDH, India) used for synthesis of inorganic material. Morphology was studied using scanning electron microscope (LEO 435 VP) and transmission electron microscope (Philips EM-400). XRD measurements were carried out on Philips PW 1148/89 diffractometer. UV/VIS spectrophotometer-Elico (India), model EI 301E;a double beam atomic absorption spectrophotometer (GBC 902, Australia); a thermal analyzer-V2.2A DuPont 9900; Carlo-Erba, model 1108; a digital potentiometer (Equiptronics EQ 609, India); accuracy ±0.1 mV with a saturated calomel electrode as reference electrode; an electronic balance (digital, Sartorius-21OS, Japan) and an automatic temperature controlled water bath incubator shaker-Elcon (India) were used for carrying out instrument.

Synthesis of Polymer

A typical procedure to prepare PMMA was followed which involved placing 20 mL of MMA, 0.15 g (0.75%) of BPO in 100 mL of water, and 0.5 g of PVA and 5 g of di-sodium hydrogen phosphate in a 250 mL three-necked round bottom flask and the solution was stirred for 1 h at 80°C to complete the polymerization of monomer. Nitrogen was bubbled into the flask throughout the reaction. The solution was then filtered, washed, and finally dried for 24 h at 100°C. Spherical beads of PMMA obtained.

Synthesis of PMMA–$CeMoO_4$ Composite. The same procedure was followed except after half an hour of reaction the inorganic sol was added. Inorganic precipitate of Ce (IV) molybdate was prepared by mixing aqueous solutions of 0.1*M* ceric ammonium nitrate and 0.1*M* ammonium molybdate in different volume ratios at room temperature (25°C ± 2°C) as mentioned in Table I. The white precipitates were obtained when the pH of the mixtures was adjusted to 1.0 by adding aqueous ammonia or hydrochloric acid with constant stirring. Furthermore, this homogeneous mixture was added drop wise over 30 min into the reaction media of monomers with rigorous stirring to avoid local inhomogeneities. The supernatant liquid was decanted and gels were filtered under suction. The excess acid was removed by washing with DMW and the material was dried under vacuum at 50°C. They were converted to H^+-form by treating with 1*M* HNO_3 for 24 h with occasional shaking, intermittently replacing the supernatant liquid with fresh acid. Washings with DMW removed the excess acid and then dried at 50°C. Because of high ion-exchange capacity sample S-6 was selected for carrying out further studies.

Ion-Exchange Capacity

Alkali (1*M*) and alkaline earth metal nitrates were used as eluants to elute the H^+ ions completely from one gram (1 g) of the dry cation-exchanger by column method, maintaining a very slow flow rate (~0.5 mL/min). The effluent was titrated against a standard (0.1*M*) NaOH solution for the total ions liberated in the solution using phenolphthalein as indicator and I.E.C. (mequiv/g) values were noted.

Thermal Effect on Ion-Exchange Capacity

To study the effect of drying temperature on ion-exchange capacity, 1.0 g samples of the composite cation-exchange material in H^+-form were heated at various temperatures in a muffle furnace for 1 h and the Na^+ ion-exchange capacity was determined by column process after cooling them at room temperature.

Table II. Ion-Exchange Capacity of Various Exchanging Ions on PMMA–CeMoO4 Column

Exchanging metal ions	pH of the metal solution	Ionic radii (Å)	Hydrated ionic radii (Å)	Ion-exchange capacity (mequiv/g)
Li^+	6.9	0.68	3.40	0.88
Na^+	6.30	0.97	2.76	1.60
K^+	6.2	1.33	2.32	1.77
Mg^{2+}	6.0	0.78	7.00	1.85
Ca^{2+}	6.5	1.06	6.30	2.01
Sr^{2+}	6.3	1.27	-	2.76
Ba^{2+}	6.2	1.43	5.90	3.12

Regeneration of Ion Exchanger

Exhausted exchanger was regenerated by keeping it overnight in hydrochloric acid (0.1*M*). It was then washed with DMW, till it became neutral. The exchange capacity was determined. This procedure was repeated five times and it was observed that after five regenerations, ion exchanger loses 40% of its original capacity.

Characterization of Hybrid Composite Material

The nature, particle size, morphology, thermal stability, and the functional groups present in the prepared composite material has been characterized by using TEM, SEM, XRD, FTIR, and TGA-DTA techniques.

Selectivity (Sorption) Studies

The distribution behavior of metal ions plays an important role in the determination of the material's selectivity. In certain practical applications, equilibrium is most conveniently expressed in terms of the distribution coefficients of the counter ions.

The determination of metal ions before and after equilibrium was carried out volumetrically using EDTA as titrant.[37] Two hundred milligram of the dry exchanger in H^+ form were equilibrated with 20 mL of different metal nitrate solutions in the required medium and kept for 24 h with intermittent shaking. The initial metal ion concentration (0.01*M*) was so adjusted that it did not exceed 3% of total ion exchange capacity of the material.

The distribution coefficient (K_d) values were calculated by using the formula given below:

$$K_D = [(I - F)] \times V/M(mL/g) \quad (1)$$

where "*I*" is the initial amount of metal ion in the aqueous phase, *F* is the final amount of metal ion in the aqueous phase, *V* is the volume of the solution (mL), and *M* is the amount of cation-exchanger (g).

Preparation and Characterization of Composite Membrane

The Coetzee and Benson method[38] was employed for the preparation of ion exchange membranes of PMMA–$CeMoO_4$. A number of membranes were prepared using finely grounded electroactive material, the PMMA–$CeMoO_4$ cation-exchanger, with varying amounts of binder such as Araldite (Ciba-Geigy; 100 mg) on Whatman's filter paper. A piece of membrane was cut out and fixed at one end of a Pyrex glass tube (o.d. 0.8 cm, i.d. 0.6 cm) with Araldite. Those membranes which exhibited good surface qualities, like porosity, thickness, swelling, etc., were selected for further investigations. The preparation method was same as reported[39] earlier. The membranes were conditioned for measuring swelling and water content by equilibrating with 1*M* sodium chloride; about 1 mL of sodium acetate was also added to adjust the pH to be in the range of 5–6.5 (to neutralize the excess acid present in the film).

The water content (% water uptake) was calculated as:

$$\%\text{Wateruptake} = \frac{W_w - W_d}{W_w} \times 100$$

where W_d = weight of the dry membrane and W_w = weight of the soaked/wet membrane.

EMF Measurements. Membranes were fixed to one end of a Pyrex glass tube (o.d. 1.6 cm, i.d. 0.8 cm) using araldite as adhesive. These were then equilibrated with Pb^{2+} solution (0.1*M*) for 5–7 days. The tube was filled 3/4th with $Pb(NO_3)_2$ solution (0.1*M*) and then immersed in a beaker containing the test solution of varying concentration of Pb^{2+}ion, keeping the level of inner filling solution higher than the level of the test solution to avoid any reverse diffusion of the electrolyte. All the EMF measurements were carried out using the following cell assembly:

SCE|0.1*M* Pb^{2+}||Membrane||0.1*M* Pb^{2+} (test solution)|SCE

Potentiometric measurements were observed for a series of standard solutions of Pb $(NO_3)_2$ (10^{-10}–10^{-1}*M*), prepared by gradual dilution of the stock solution, as described by IUPAC Commission for Analytical Nomenclature.[40] Potential measurements were made in unbuffered solutions to avoid interference from any foreign ion. The calibration graphs were plotted three times to check the reproducibility of the system.

Characteristics of the Electrode. To study the characteristics of the electrode, the following parameters were evaluated: lower detection limit, slope response curve, response time and

Table III. Effect of Temperature on Ion Exchange Capacity of PMMA–CeMoO4 Composite Cation Exchanger for 1 h

Heating temperature in (°C)	Appearance (color)	% Weight loss	Na^+ ion-exchange capacity (mequiv/g)	% Retention of I.E.C.
50	Pale yellow	-	1.60	100
100	Pale yellow	1.2	1.60	100
150	Pale yellow	2.7	1.59	94
200	Cream color	4.4	1.38	75.62
250	Cream color	5.0	1.27	65.62
300	Dirty white	5.5	1.15	53.75
350	Dirty white	7.0	1.06	12.5
400	Dirty white	24	0.76	6.8
500	White	42.2	0.20	1.8
600	White	47.5	0.11	1.8
700	White	49	0.03	0

working pH range. In the present study, the selectivity coefficient was calculated by fixed interference method, which is one of the mixed solution methods[41] using the equation given below:

$$K_{AB}^{\text{pot}} = a_A/(a_B)^{zA/zB}$$

where a_A and a_B are the activities of primary and interfering ion having charges z_A, z_B.

Storage of Electrodes. The polyaniline-based composite electrode was stored in distilled water when not in use for more than 1 day. It was activated with (0.1*M*) Pb^{2+} solution by keeping immersed in it for 2 h, before use, to compensate for any loss of metal ions in the membrane phase that might have taken place due to a long storage in distilled water. Electrode was then washed thoroughly with DMW before use.

Analytical Application of the Electrode. The analytical utility of this membrane electrode has been established by employing it as an indicator electrode in the potentiometric titration of a 0.01*M* Pb $(NO_3)_2$ solution against 0.005*M* EDTA solution and 0.005*M* $Pb(NO_3)_2$ was titrated with 0.01*M* oxalic acid. Potential values are plotted against the volume of EDTA/Oxalic acid.

RESULTS AND DISCUSSION

PMMA has extra methyl groups acting like the spikes to put a quick stop to any slithering. PMMA can be produced using a variety of polymerization mechanisms. The German chemists Fittig and Paul discovered in 1877 the polymerization process that turns methyl methacrylate into poly(methyl methacrylate).

The most common technique is the free radical polymerization of MMA.[42,43] The free radical polymerization of MMA can be performed homogeneously, by bulk or solution polymerization, or heterogeneously, by suspension or emulsion polymerization. Small beads of PMMA can be readily produced using suspension polymerization. Suspension polymerization is initiated with free radical initiators that favor the monomer phase, such as benzoyl peroxide and dispersant, like polyvinyl alcohol (PVA), which stabilize the polymerization and prevent the droplets from adhering to one another. The mechanism is given below:

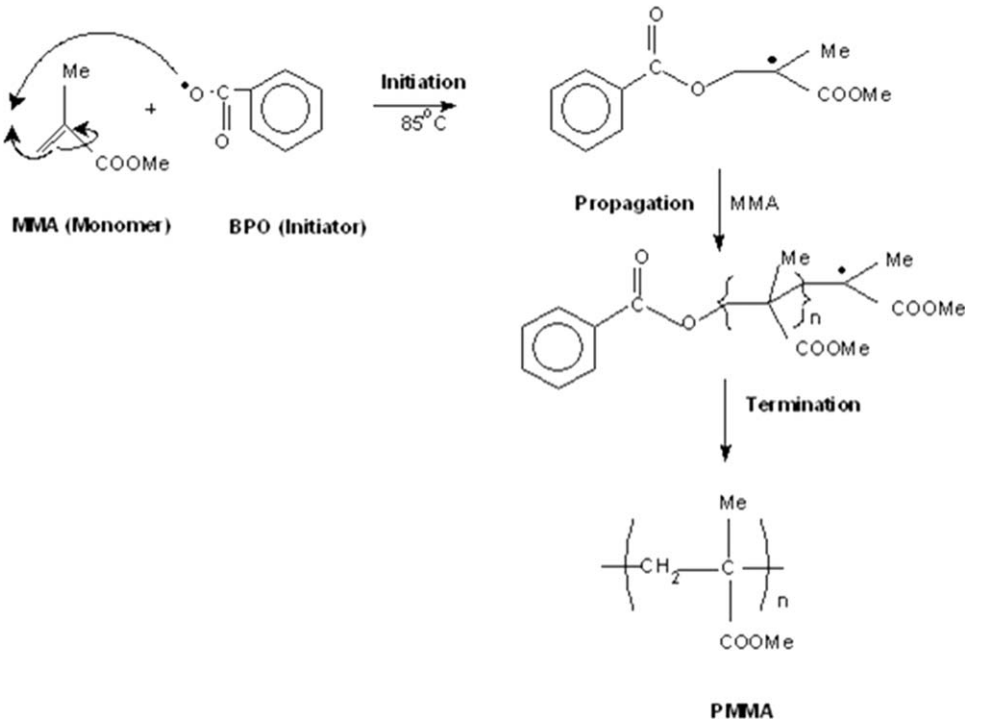

The binding of polymer into the inorganic matrix can be explained as:

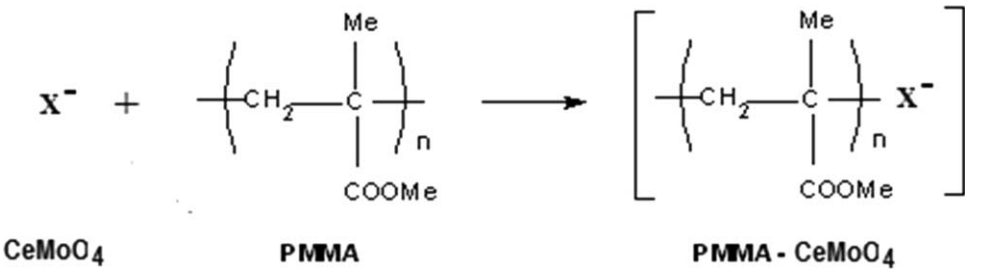

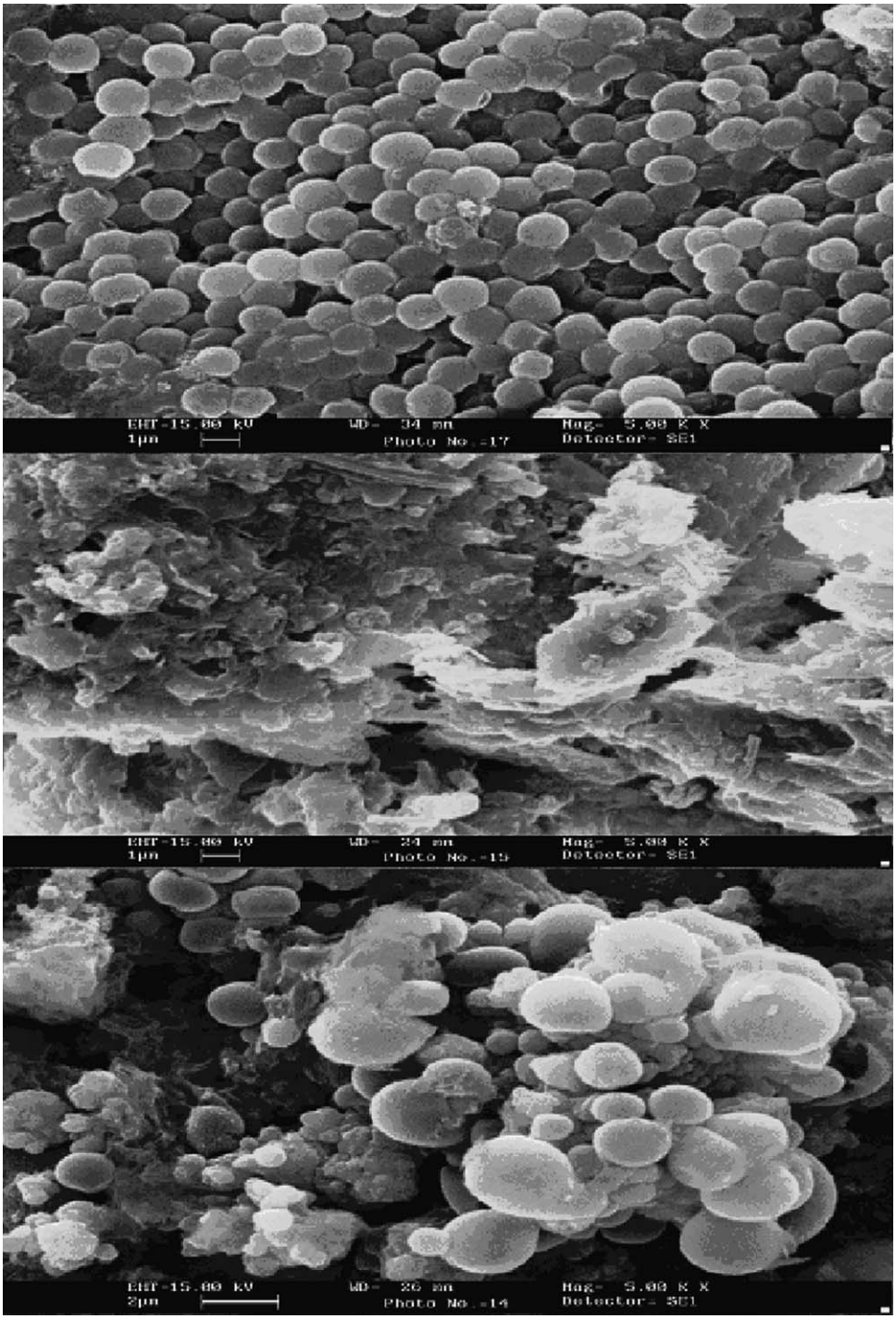

Figure 1. Scanning electron microphotographs of chemically prepared (a) PMMA, (b) $CeMoO_4$, and (c) PMMA–$CeMoO_4$ composite system.

Thereby, organic–inorganic composite of PMMA–$CeMoO_4$ was obtained having good ion exchange capacity (Table I). To check the reproducibility of prepared composite, it was synthesized five times under identical conditions of concentration of reagents, mixing ratio and drying temperature. The composition and ion exchange capacity and yield of each product were examined. The averages and standard deviation of the ion exchange capacity and yield were found to be 1.60 mequiv/g and $\pm$0.03%, respectively.

The effect of the size and charge of the exchanging ion on the ion-exchange capacity was also observed for this material. The alkali metals shows a decreasing trend for the ion exchange capacity ($K^+ > Na^+ > Li^+$) whereas the alkaline earth metal ions follow the order $Ba^{2+} > Sr^{2+} > Ca^{2+} > Mg^{2+}$. The size and

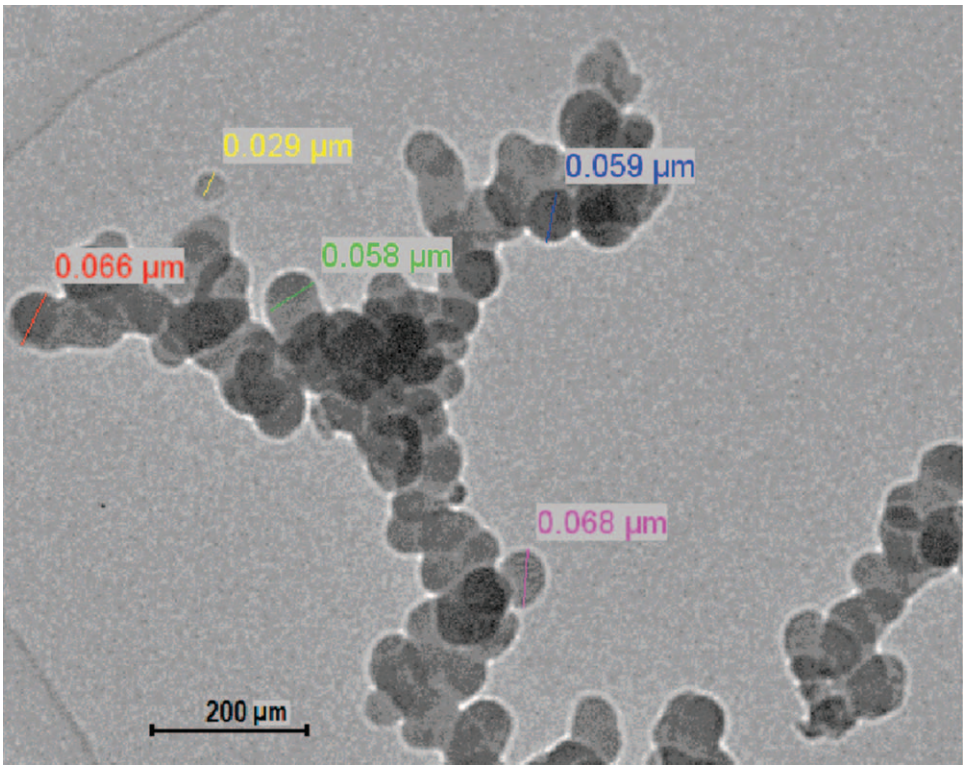

Figure 2. TEM of PMMA–$CeMoO_4$ showing different particle size. [Color figure can be viewed in the online issue, which is available at wileyonlinelibrary.com.]

charge of the exchanging ions affect the ion exchange capacity of exchanger.[44,45] This sequence is in accordance with the hydrated radii of the exchanging ions (Table II). Ions with the smaller hydrated radii easily enter the pores of the exchanger, which results in higher adsorption. According to Kossel,[46] Goldschmidt,[47] and Pauling[48] the attraction between cations and anions in ionic crystals obey Coulomb's law on demands for ions of equal charge, a small ion will be attracted either to a greater force or held more tightly than a larger ion. Therefore,

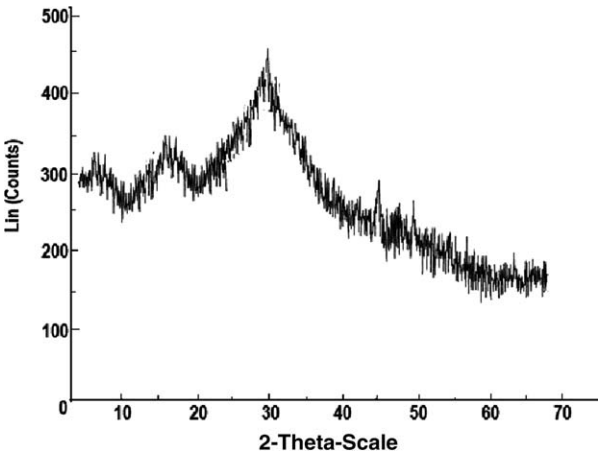

Figure 3. Powder X-ray diffraction pattern of PMMA–$CeMoO_4$ (as prepared).

the ion-exchange capacity should increase with decreasing hydrated radii and increase with electric potential.

The superiority of the newly synthesized material PMMA–$CeMoO_4$ can be readily emphasized from good thermal stability as it maintained 58% of its mass by heating up to 500°C. The weight loss starts from 100°C but in respect to the ion-exchange capacity and appearance, the material was found highly stable (Table III) up to 150°C and it retained about 65% of its ion–exchange capacity and 95% of its initial mass without noticeable change in color and physical appearance till 250°C. It may be due to the loss of external water molecule and condensation of material. The results support the TGA studies.

A study was performed to examine the difference in surface morphology between the parent materials and their composites. Figure 1 illustrates the micrographs of scanning electron microscopy (SEM) revealing that their production was successfully achieved yielding materials with particles well dispersed. Figure 1(a) shows the micrograph of virgin polymers and it can be seen that the distribution of size was not uniform and the particles size varies. Their chain formation is clearly visible from the micrograph. In Figure 1(c), SEM picture shows $CeMoO_4$ adhered to the polymer surface. There are some agglomerates formed which are reflected as larger particles.

The TEM micrograph shows the particle size of "polymeric-inorganic" composite PMMA–$CeMoO_4$. The composite's particle size lies in the range of 1-100 nm (Figure 2) which proves

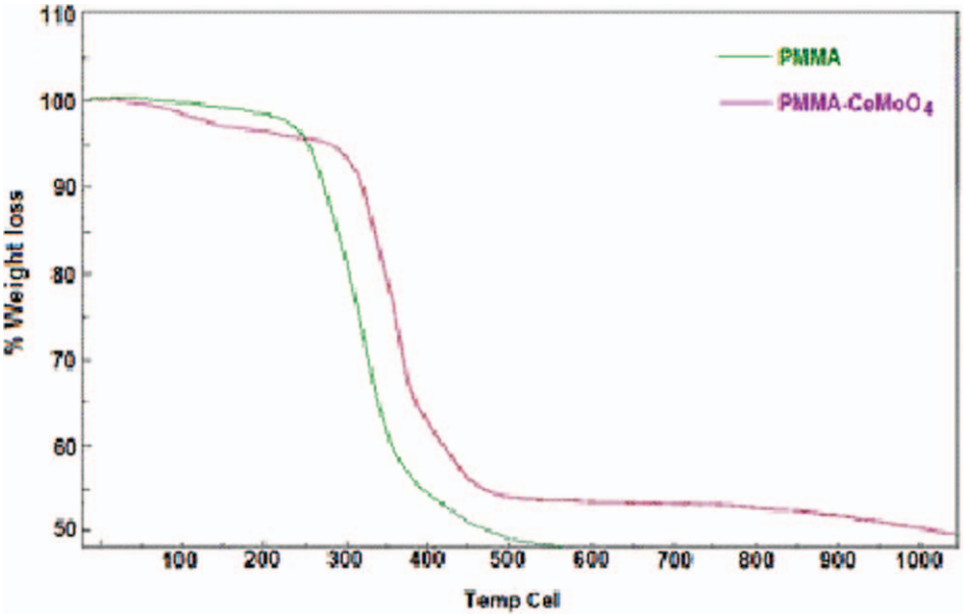

Figure 4. Simultaneous TGA curves of PMMA and PMMA–$CeMoO_4$ (as prepared). [Color figure can be viewed in the online issue, which is available at wileyonlinelibrary.com.]

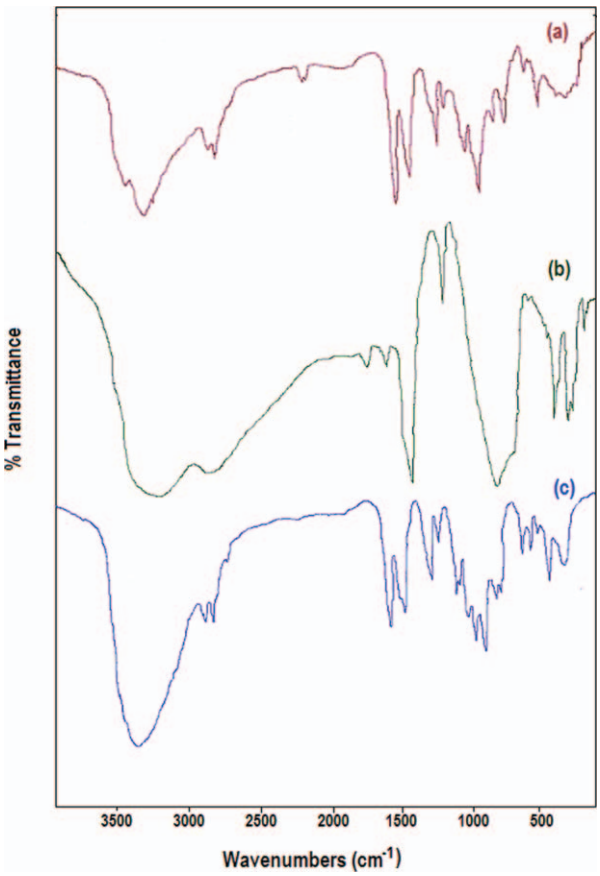

Figure 5. FTIR spectra of as prepared (a) PMMA, (b) $CeMoO_4$, and (c) PMMA–$CeMoO_4$. [Color figure can be viewed in the online issue, which is available at wileyonlinelibrary.com.]

that the prepared cation exchanger PMMA–$CeMoO_4$ is a nanocomposite.

The X-ray diffraction studies of the composite cation-exchanger (S-6; as prepared) was carried out using Rigaku X-Ray powder diffractometer with Cu anode (K_α $\lambda = 1.54186$Å) in the range of $5° \leq 2\theta \leq 70°$ at 30 kV. Figure 3 shows the typical XRD pattern of the sample at room temperature. It is evident from the XRD pattern that the material is formed in the semicrystalline phase. The XRD pattern matches with the peaks of $CeMoO_4$and PMMA[50] as reported. PMMA is known to be an amorphous polymer.[51] The addition of $CeMoO_4$ does not induce any crystallinity in these polymers. This also explains the homogeneous nature of composite material. The suppositions of peaks confirm the nature and formation of the synthesized composite.

Figure 4 compare the thermal property of polymer PMMA to that of PMMA–$CeMoO_4$ composite. The loss of weight started around 250°C onward which indicated the depolymerization of polymer. On the contrary, the start of depolymerization was retarded in the composite. The TGA curve (Figure 4) of the composite shows loss of weight started around 350°C which was about 100°C higher than the organic polymer. The TGA curve (Figure 4) of the composite PMMA–$CeMoO_4$ shows that up to 300°C only 7% weight loss was observed which may be due to the removal of external H_2O molecules present at the surface of the composite materials.[52] A steep weight loss in PMMA–$CeMoO_4$ composite was observed between 300°C to 450°C due to conversion of inorganic molybdate. From 550°C onwards, a smooth horizontal line represents the complete formation of the oxide form of the material.

Figure 5 depicts the FT–IR spectra of PMMA, $CeMoO_4$, and PMMA– $CeMoO_4$. It is evident that all the three spectra are similar except for a few changes in the spectra of the

Table IV. Kd Values of Some Metal Ions on PMMA–CeMoO4 Composite Cation Exchanger Column in Different Solvent System

Metal ions	Ionic radii (A°)	DMW	$10^{-2}M$ HNO_3	$10^{-3}M$ HNO_3	$10^{-4}M$ HNO_3	$10^{-3}M$ H_2SO_4	$10^{-4}M$ H_2SO_4	$10^{-3}M$ HCl	$10^{-3}M$ $HClO_4$	Buffer pH 3.75	Buffer pH 5.75	Buffer 10
Mg^{2+}	0.65	148	262	298	315	156	167	184	317	178	231	200
Cu^{2+}	0.92	344	197	218	336	78	101	244	155	282	186	136
Cd^{2+}	0.97	398	322	379	422	218	255	190	243	290	106	380
Co^{2+}	0.72	415	TA	527	560	367	380	221	260	316	177	292
Sr^{2+}	1.18	270	180	236	248	304	323	116	217	246	153	130
Ca^{2+}	1.00	561	375	290	328	334	349	184	162	411	219	190
Mn^{2+}	0.80	367	-	-	112	147	238	76	214	320	117	229
Pb^{2+}	**1.18**	**1710**	**1290**	**1600**	**TA**	**593**	**614**	**580**	**934**	**1204**	**875**	**568**
Hg^{2+}	1.02	744	555	604	722	427	488	377	600	779	568	435
Al^{3+}	1.87	231	323	358	445	213	245	152	161	332	132	308
Ni^{2+}	0.69	639	417	420	442	254	225	134	239	-	330	126
Cr^{3+}	0.76	486	287	301	268	196	175	190	311	280	168	200
Zn^{2+}	0.75	702	345	428	448	-	96	217	174	348	235	120
Fe^{3+}	0.63	466	270	356	364	156	173	267	334	407	134	166

nanocomposites. The features that are similar identify the presence of PMMA in all of them. The absorption bands at 3440 cm^{-1}, 1732 cm^{-1}, and 1149–1242 cm^{-1}can be associated with –OH stretching of the lattice water, C=O stretching, and C–O stretching, respectively. The bands between 3000–2900 cm^{-1} correspond to the C–H stretching of the methyl group (CH_3) whereas the bands at 1300 and 1450 cm^{-1} are associated with C–H symmetric and asymmetric stretching modes, respectively. C–C stretching bands are at 1000 and 800 cm^{-1}. FTIR spectrum of PMMA–$CeMoO_4$ [Figure 5(c)], indicates a broad band in the region 3200–3500 cm^{-1}. These bands justify the presence of –OH stretching and bending mode (a characteristic feature of lattice water).[53] The assemblies of peaks at 950–1100 cm^{-1} in PMMA–$CeMoO_4$ are due to the presence of molybdate ions.[54] The band with maxima at 900 cm^{-1} is attributed to M–O–H bending mode, i.e., overlapping of the molybdate ion and Ce $(OH)^{2+}$, respectively. These characteristic stretching frequencies are also in close resemblance with the inorganic cation-exchanger $CeMoO_4$ which indicates that the PMMA molecules were indeed grafted on the surface of inorganic particles. All the three spectra indicate (i) the purity of the polymer obtained and (ii) formation of the nanocomposites.

The results of sorption studies (Table IV) indicated that K_d values varied with the nature and composition of contacting solvents. Three Main factors that affect the distribution coefficient of an ion to compete effectively with one another are the charge on the ion, its ionic radius and the hydrated energy of the competing ion. For an ion to be effective in a competition reaction its charge and hydration energy must be high and its radius should be small. It was observed from the distribution studies (K_d values) that the $Pb^{2+}$was highly adsorbed in all solvents, while remaining metal ions were poorly adsorbed. The high uptake of lead ions in all solvents demonstrates not only the ion-exchange properties but also the adsorption and ion-selective characteristics of the cation-exchanger.

On this basis, PMMA–$CeMoO_4$ has been used as an electroactive component in the preparation of the heterogeneous solid-state electrode sensitive to Pb^{2+} ions. Ion-selective electrodes work on the principle of measurements at zero current. The membranes were fixed in the electrode assembly and all measurements are made in a concentration cell. The concentration of the electrolyte on the inner side of the membrane was fixed at $0.1M$ of Pb^{2+}ions while outer solution varied from $10^{-12}M$ to $10^{-1}M$. When ions penetrated the boundary between the two

Table V. Characterization of Ion-Exchanger Membranes of PMMA–CeMoO4

S. no.	Membrane composition		Characterization of membrane						
	PMMA–$CeMoO_4$ (%)	Binder (%)	Thickness (mm)	% Total wet weight	Porosity	% Swelling	Slope (mV/decade)	Working range (M)	Response time (s)
M1	**10**	**Araldite (10)**	**0.30**	**0.821**	**0.00136**	**0.5620**	**29.48**	**1×10^{-9} to 1×10^{-1}**	**08**
M2.	20	Araldite (10)	0.45	1.110	0.00439	1.1511	29.02	5×10^{-8} to 1×10^{-2}	10
M3.	25	Araldite (10)	0.64	1.367	0.00730	1.6536	28.74	1×10^{-8} to 1×10^{-1}	22
M4.	30	Araldite (10)	0.72	1.780	0.00816	1.9728	28.14	1×10^{-7} to 1×10^{-1}	20

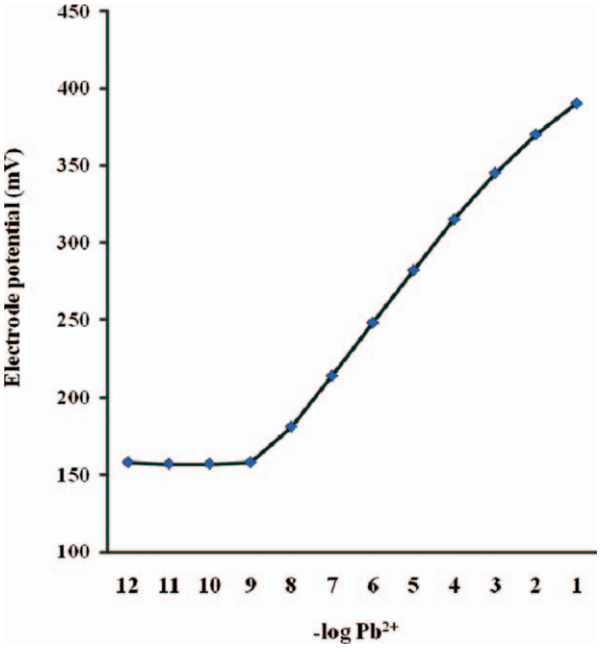

Figure 6. Calibration curve for PMMA–$CeMoO_4$ membrane (M-1) electrode in aqueous solution of $Pb(NO_3)_2$. [Color figure can be viewed in the online issue, which is available at wileyonlinelibrary.com.]

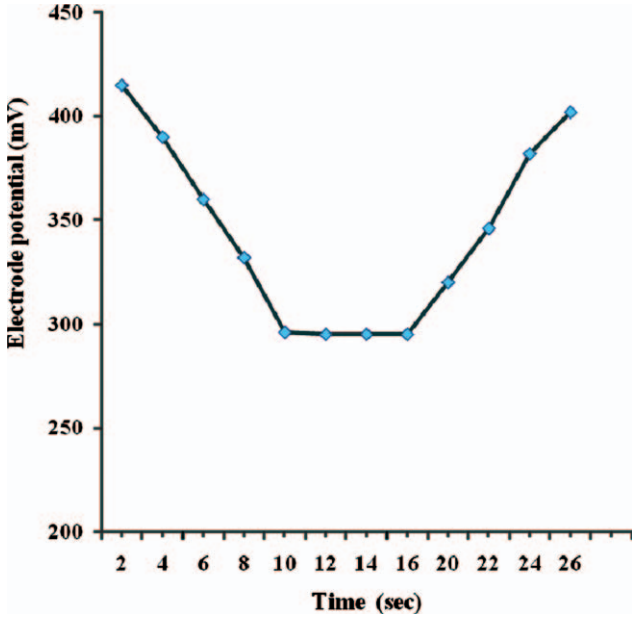

Figure 8. Dynamic response time of PMMA–$CeMoO_4$ electrode for Pb^{2+} ions. [Color figure can be viewed in the online issue, which is available at wileyonlinelibrary.com.]

phases leading to the attainment of electrochemical equilibrium, the potentials developed.

Optimization of Membrane Ingredients

It is well known that the sensitivity, linear dynamic range, and selectivity of the ISEs depend not only on the nature of the carrier used, but also significantly on the membrane composition, properties of the additives employed as well as the adhesive/plasticizer ratio used.[55] It should be noted that plasticizer acts as membrane solvent affecting membrane selectivity and also provide mobility of the membrane constituents within the membrane phase. In the present study, dioctylphthalate was used as plasticizer. Influence of the membrane composition and possible interfering ions was investigated on the response properties of the electrode. The slope of the calibration curve, the measurement range and response time were noted for a number of electrodes. The results are shown in Table V and membrane electrode no.1 (M-1) was chosen for further electroanalytical studies. The low order of water content, the swelling, porosity and lesser thickness of these membranes suggest that interstices are negligible and diffusion across the membranes would occur mainly through the exchanger sites.

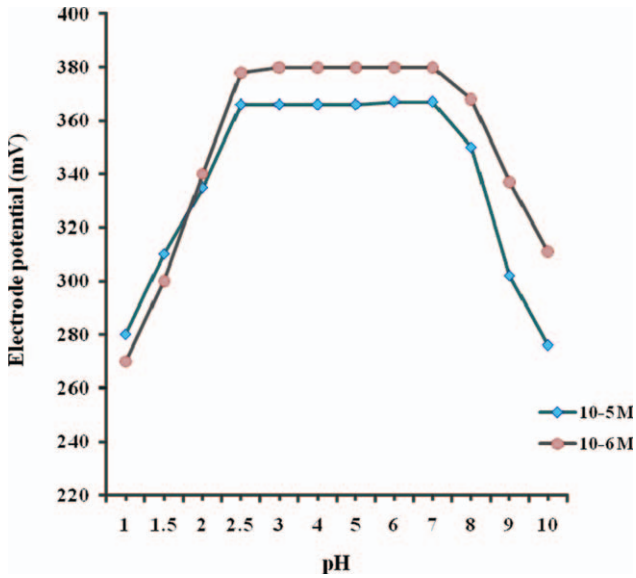

Figure 7. The influence of pH on the potential response of the membrane electrode at 1×10^{-5} and $1 \times 10^{-6} M$ Pb^{2+} ion. [Color figure can be viewed in the online issue, which is available at wileyonlinelibrary.com.]

Calibration Range

Using the optimized membrane composition described above, the potentiometric response of the sensor was studied for Pb^{2+} in the concentration range of $10^{-12} M$ to $10^{-1} M$ at 25°C as shown in Figure 6. The results showed a Nernstian response of 29.48 mV/decade of Pb^{2+} concentration, and the wide linear range within the concentration range from $10^{-9} M$ to $10^{-1} M$ of Pb^{2+}ions. Experiments were conducted a number of times to check the reproducibility of the results. EMFs were plotted against log of activities of lead ions and calibration curves were drawn for five sets of experiments and a standard deviation of ± 0.3 mV was observed. The detection limit of sensor was determined according to IUPAC recommendations from the intersection of two extrapolated linear portions of the curve[56] and was found to be 5×10^{-9}. To evaluate the reversibility of the electrode, a similar procedure at the opposite direction was adopted. The measurements were performed in the sequence of high-to-low sample concentrations and very similar results were obtained.

Table VI. The Stability of the Pb2+ Selective PMMA–CeMoO4 Membrane Electrode

Time (Day)	Slope (mV/decade)	Working range (*M*)
1	29.48 ± 0.2	1×10^{-9} to 1×10^{-1}
5	29.48 ± 0.2	1×10^{-9} to 1×10^{-1}
10	29.48 ± 0.2	1×10^{-9} to 1×10^{-1}
15	29.48 ± 0.2	1×10^{-9} to 1×10^{-1}
30	29.35 ± 0.4	1×10^{-9} to 1×10^{-1}
50	29.22 ± 0.2	1×10^{-9} to 1×10^{-1}
70	29.18 ± 0.3	1×10^{-9} to 1×10^{-1}
90	29.11 ± 0.3	1×10^{-9} to 1×10^{-1}
120	29.07 ± 0.4	1×10^{-9} to 1×10^{-1}
150	29.0 ± 0.05	1×10^{-9} to 1×10^{-1}
180	28.86 ± 0.03	5×10^{-8} to 1×10^{-1}
210	28.41 ± 0.4	5×10^{-8} to 1×10^{-1}
240	28.20 ± 0.4	1×10^{-8} to 1×10^{-1}

Response, Reproducibility, and Lifetime

The influence of pH of the test solution on the potential response of the membrane sensor was investigated over a pH range of 1–12. The pH was adjusted with dilute hydrochloric acid and sodium hydroxide solutions as required. The influence of pH on the response of the membrane sensor is shown in Figure 7. The results showed that the potential is independent of pH in the range of 2.5 to 6.0, beyond which the potential changes considerably. The dependency of the potential to the pH values out of this range can be attributed to the formation of some hydroxyl complexes of lead (II) ion[57] at higher pH values and to the hydrogen ion response at lower pH values.

For analytical applications, the response time of a sensor is an important factor. The response time for the Pb^{2+}-selective electrode to attain a response that is within ±1 mV of steady state potential after successive immersion of the electrodes in a series of lead solutions, each having a 10-fold difference in concentration from $10^{-4}M$ to $10^{-5}M$ was investigated. The electrode showed reasonably fast and stable potential within 8 s and no change was normally observed up to 5 min after which it started deviating (Figure 8).

Table VII. The Selectivity Coefficient of Various Interfering Cations for Pb2+ Selective PMMA–CeMoO4 Membrane Electrode

Interfering ion (M^{n+})	Selectivity coefficients (K_{MSM})
K^+	0.045
Na^+	0.062
Mg^{2+}	0.0086
Cu^{2+}	0.0055
Hg^{2+}	0.0040
Ca^{2+}	0.0021
Al^{3+}	0.052
Sr^{2+}	0.022
Mn^{2+}	0.025
Fe^{3+}	0.072
Ni^{2+}	0.00072
Zn^{2+}	0.0012
Cd^{2+}	0.0047

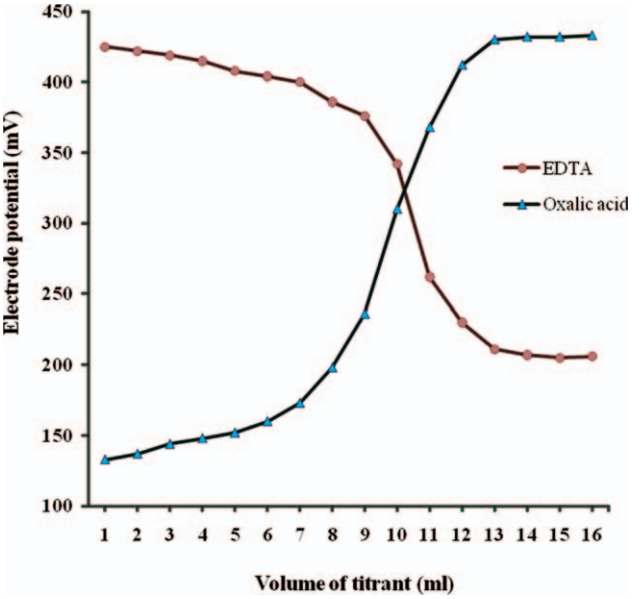

Figure 9. Application of the electrode based on PMMA–$CeMoO_4$ for potentiometric titration of (a) 0.01*M* $Pb(NO_3)_2$ with 0.005*M* EDTA and (b) 0.005*M* $Pb(NO_3)_2$ with 0.01*M* oxalic acid. [Color figure can be viewed in the online issue, which is available at wileyonlinelibrary.com.]

The long-term stability was worked out by performing calibrations periodically with standard solutions and calculating the slopes over the concentration ranges of $10^{-10}M$ to $10^{-1}M$ of Pb $(NO_3)_2$ solutions over a period of 240 days. During this period, the electrodes were in daily use over an extended period of time (1 h per day), and the results are provided in Table VI. The experimental results showed that the electrode response was quite reproducible over the lifetime of 150 days (Table VI) after that a very slight gradual decrease in the slopes and working range was observed. Subsequently, the electrochemical behavior of the sensor gradually deteriorated which may be due to ageing of the adhesive (araldite), the plasticizers, and the electroactive material.[58] A decrease in slope was a symptom of loss of the normal characteristics of the electrodes.

Potentiometric Selectivity

One of the important characteristics of the ion-selective electrode is its selectivity which determines whether reliable measurement in the target sample is possible or not. To assess the selectivity preference of the membrane for an interfering ion relative to Pb^{2+} was determined by the mixed solution method (MSM). It is evident from Table VII, most of the interfering ions showed low values of selectivity coefficient, indicating no interference in the performance of the membrane electrode assembly. Such remarkable selectivity of the proposed ion-selective electrode over other ions reflects the high affinity of the membrane toward the lead ions.

Analytical Application

The sensor was successfully applied as indicator electrodes in the potentiometric titration of Pb^{2+} ion solution with EDTA

and oxalic acid. The addition of titrants causes a decrease in potential as a result of decrease in free Pb^{2+} ion concentration due to formation of a complex with EDTA/oxalic acid (Figure 9). The titration curves showed good inflection point at the equivalence point, showing perfect stoichiometry. Titration curve "A" represents the decreasing trend of potential response, on addition of lower volume of the titrant to the higher volume of it, and the curve "B" represents *vice versa*.

CONCLUSION

The proposed potentiometric sensor of nanocomposite cation exchanger, PMMA–$CeMoO_4$, has good operating characteristics including Nernstian response, reasonable detection limit, relatively high selectivity, wide dynamic range and fast response. These characteristics and the typical applications presented in this paper make the sensor a suitable for measuring Pb (II) content in real samples without a significant interaction from cationic or anionic species. A comparison between the response characteristics of the proposed potentiometric sensor and those of previously reported lead ion-selective electrode indicated that the present sensor is invariably superior.

ACKNOWLEDGMENTS

The authors acknowledge the Department of Applied Chemistry, Z.H. College of Engineering and Technology, A.M.U. (Aligarh) for providing research facilities. They are highly thankful to Dr. A. Azam (Reader), Department of Applied Physics, A.M.U. for his valuable support and suggestion to carry out XRD analysis and also acknowledged the technical assistance provided by the AIIMS and I.I.T. Roorkee. The authors are grateful for the financial support provided by Ministry of Environment & Forest, Government of India.

REFERENCES

1. Novak, B. M. *Adv. Mater.* **1993,** *5*, 422.
2. Schubert, U.; Husing, N.; Lorenz, A. *Chem. Mater.* **1995,** *7*, 2010.
3. Wen, J.; Wilkes, G. L. *Chem. Mater.* **1996,** *8*, 1667.
4. Lee, D. C.; Jang, L. W. *J. Appl. Polym. Sci.* **1996,** *61*, 1117.
5. Beecroft, L. L.; Ober, C. K. *Chem. Mater.* **1997,** *9*, 1302.
6. Wei, Y.; Wang, W.; Yeh, J. M.; Wang, B.; Yang, D.; Murray, J. K., Jr. *Adv. Mater.* **1994,** *6*, 372.
7. Wei, Y.; Jin, D.; Yang, C. C.; Wei, G. J. *Sol. Gel Sci. Tech.* **1996,** *7*, 191.
8. Wei, Y.; Jin, D.; Brennan, D. J.; Rivera, D. N.; Zhuang, Q.; DiNardo, N. J.; Qiu, K. *Chem. Mater.* **1998,** *10*, 769.
9. Wang, Q.; Liu, N.; Wang, X.; Li, J.; Zhao, X.; Wang, F. *Macromolecules* **2003,** *36*, 5760.
10. Matsuura, Y.; Miura, S.; Naito, H.; Inoue, H.; Matsukawa, K. J. *Organomet. Chem.* **2003,** *685*, 230.
11. Chujo, Y.; Matsuki, H.; Kure, S.; Saegusa, T.; Yazawa, T. J. *Chem. Soc. Chem. Commun.* **1994, 635.**
12. Tamaki, R.; Samura, K.; Chujo, Y. *Chem. Commun.* **1998**, 1131.
13. Tamaki, R.; Chujo, Y. *Chem. Mater.* **1999,** *11*, 1719.
14. Ogoshi, T.; Chujo, Y. *Macromolecules* **2004,** *37*, 5916.
15. Ogoshi, T.; Itoh, H.; Kim, K. M.; Chujo, Y. *Macromolecules* **2002,** *35*, 334.
16. Khan, A. A.; Akhtar, T. *Electrochim. Acta* **2009,** *54*, 3320.
17. Khan, A. A.; Paquiza, L.; Khan, A. J. *Mater. Sci.* **2010,** *45*, 3610.
18. Khan, A. A.; Khan, S. A.; Siddiqui, W. A. *Talanta* **2007,** *71*, 841.
19. Khan, A. A.; *Inamuddin. React. Funct. Polym.* **2006,** *66*, 1649.
20. Khan, A. A.; Alam, M. M. *Anal. Chim. Acta* **2004,** *504*, 253.
21. Khan, A. A.; Alam, M. M. *React. Funct. Polym.* **2003,** *55*, 277.
22. Petrucci, M.; Fenwick, D.; Kakkar, A. J. *Mol. Catal. A: Chem.* **1999,** *146*, 309.
23. Dallmann, K.; Buffon, R. *Catal. Commun.* **2000,** *1*, 9.
24. Guizard, C.; Bac, A.; Barboiu, M.; Hovnanian, N. *Sep. Purif. Technol.* **2001,** *25*,167.
25. Iwata, M.; Adachi, T.; Tonidokoro, M. J. *Appl. Polym. Sci.* **2003,** *88*, 1752.
26. Jung, D. H.; Cho, S. Y.; Pech, D. H. *J. Power Sources* **2002,** *106*, 173.
27. Honma, I.; Nishikawa, O.; Sugimoto, T.; Nomura, S.; Nakajima, H. *Fuel Cells* **2002,** *2*, 52.
28. Barboiu, M.; Luca, C.; Guizard, C. J. *Membr. Sci.* **1997,** *129*, 197.
29. Barboiu, V.; Barboiu, M. J. *Membr. Sci.* **2002,** *204*, 97.
30. Ahmadi, S. J.; Huang, Y. D.; Li, W. J. *Mater. Sci.* **2004,** *39*, 1919.
31. Huang, Z. H.; Oiu, K. Y. *Polym. Bull.***1995,** *35*, 607.
32. Wang, H. T.; Xu, P.; Zhong, W.; Shen, L.; Du, Q. *Polym. Degrad. Stab.* **2005,** *87*, 319.
33. Abbaspour, A.; Tavakol, F. *Anal. Chim. Acta* **1999,** *378*,145.
34. Sadeghi, S.; Dashti, R. Z.; Shamsipur, M. *Sensors Actuat. B* **2002,** *81*, 228.
35. Rouhollahi, A.; Ganjali, M. R.; Shamsipur, M. *Talanta* **1998,** *46*,1346.
36. Mousavi, M. F.; Barzegar, M. B.; Sahari, S. *Sensors Actuat. B* **2001,** *73*, 204.
37. Reiliy, C. N.; Schmidt, R. W.; Sadek, F. S. *J. Chem. Ed.* **1959,** *36*, 555.
38. Coetzee, C. J.; Benson, A. J. *Anal. Chim. Acta* **1971,** *57*, 478.
39. Khan, A. A.; Khan, A.; *Inamuddin. Talanta* **2007,** *72*, 699.
40. Recommendation for publishing manuscripts on ion-selective electrodes (prepared for publication by G.G. Guilbault), Commission on Analytical Nomenclature, Analytical chemistry Division, IUPAC, Ion-Sel El Rev **1969, 1.**
41. Jain, A. K.; Singh, R. P.; Bala, C. *Anal. Lett.* **1982,** *15*, 1557.
42. Stickler, M.; Rhein, T. Polymethacrylates. Ullmann's Encyclopedia of Industrial Chemistry, 5th ed.; VHS: New York, **1992,** *A21*.
43. Kine, B. B.; Novak, R. W. Encyclopedia of Polymer Science and Engineering; Wiley: New York, **1985, 262.**
44. Gupta, A. P.; Agarwal, H.; Ikram, S. J. *Ind. Chem. Soc.* **2003,** *80*, 57.

45. Rawat, J. P.; Singh, J. P. *Can. J. Chem.* **1976,** *54*, 2534.
46. Kossel, W. *Am. Phys.* **1916,** *49*, 222.
47. Goldschmidt, V. M. *Trans. Faraday Soc.* **1925,** *25*, 320.
48. Paulling, L. *Am. J. Chem. Soc.* **1929,** *51*, 1010.
49. Alam, Z.; Inamuddin, N. *Desalination* **2010,** *250*, 515.
50. Khan, M. S.; Khalil, U.; Nasar, G. J. *Pak. Mater. Soc.* **2009,** *3*, 22.
51. Meneghetti, P.; Qutubuddin, S. *Langmuir* **2004,** *20*, 3424.
52. Duval, C. Inorganic Thermogravimetric Analysis; Elsevier: Amsterdam, **1963,** *315*.
53. Nilchi, A.; Maalek, B.; Kanchi, A.; Maragheh, M. G.; Bagheri, A. *Radiat. Phys. Chem.* **2006,** *75*, 301.
54. Rao, C.N. R. Chemical Applications of Infrared Spectroscopy; Academic Press:New York, **1963.**
55. Huser, M.; Gehrig, P. M.; Morf, W. E.; Simon, W.; Lindner, C.; Jeney, J.; Toth, K.; Pungor, E. *Anal. Chem.* **1991,** *63*, 1380.
56. Umezawa, Y.; Umezawa, K.; Sato, H. *Pure Appl. Chem.* **1995,** *67*, 507.
57. Cotton, F. A.; Wilkinson, G. Quimica Inorganica Avanzada, 4th ed.; Limusa: Mexico, **1996,** *73*.
58. Oesch, U.; Simon, W. *Anal. Chem.* **1980,** *52*, 692.